Series Solution of the System of Integro-Differential Equations

Saeid Abbasbandy and Elyas Shivanian

Department of Mathematics, Imam Khomeini International University, Qazvin, 34149-16818, Iran

Reprint requests to S. A.; Fax: +982813780040; E-mail: abbasbandy@yahoo.com

Z. Naturforsch. **64a,** 811 – 818 (2009); received September 26, 2008 / revised January 5, 2009

This investigation presents a mathematical model describing the homotopy analysis method (HAM) for systems of linear and nonlinear integro-differential equations. Some examples are analyzed to illustrate the ability of the method for such systems. The results reveal that this method is very effective and highly promising.

Key words: Homotopy Analysis Method; Linear System of Integro-Differential Equations; Non-Linear System of Integro-Differential Equations.

1. Introduction

The homotopy analysis method [1, 2], is developed to search the accurate asymptotic solutions of nonlinear problems. This technique has been successfully applied to many nonlinear problems such as the viscous flows of non-Newtonian fluids [3, 4], the Korteweg-de Vries-type equations [5, 6], nonlinear heat transfer [7, 8], finance problems [9, 10], Riemann problems related to nonlinear shallow water equations [11], projectile motion [12], Glauert-jet flow [13], nonlinear water waves [14], groundwater flows [15], Burgers-Huxley equation [16], time-dependent Emden-Fowler type equations [17], differential-difference equation [18], Laplace equation with Dirichlet and Neumann boundary conditions [19], thermal-hydraulic networks [20], and recently for the Fitzhugh-Nagumo equation [21], and so on. On the other hand, one of the interesting topics among researchers is solving integro-differential equations. In fact, integro-differential equations arise in many physical processes, such as glass-forming process [22], nanohydrodynamics [23], drop wise condensation [24], and wind ripple in the desert [25]. There are various numerical and analytical methods to solve such problems, but each method limits to a special class of integro-differential equations. El-Sayed et al. applied the decomposition method to solve high-order linear Volterra-Fredholm integro-differential equations [26]. In [27], the variational iteration method was applied to solve the system of linear integro-differential equations. Also, Biazar et al. solved a system of integro-differential equations by homotopy perturbation method and Adomian decomposition method [28, 29].

The purpose of this paper is applying the homotopy analysis method to solve the system of general nonlinear integro-differential equations which is as follows:

$$\begin{aligned}
&u_1^{(m)}(x) = \\
&H_1\big(x, u_2(x), \ldots, u_2^{(m)}(x), \ldots, u_n(x), \ldots, u_n^{(m)}(x)\big) \\
&+ \int_a^b W_1\big(x, t, u_1(t), \ldots, u_1^{(m)}(t), \ldots, u_n(t), \ldots, u_n^{(m)}(t)\big)\,\mathrm{d}t \\
&+ \int_0^x K_1\big(x, t, u_1(t), \ldots, u_1^{(m)}(t), \ldots, u_n(t), \ldots, u_n^{(m)}(t)\big)\,\mathrm{d}t, \\
&u_2^{(m)}(x) = \\
&H_2\big(x, u_1(x), \ldots, u_1^{(m)}(x), \ldots, u_n(x), \ldots, u_n^{(m)}(x)\big) \\
&+ \int_a^b W_2\big(x, t, u_1(t), \ldots, u_1^{(m)}(t), \ldots, u_n(t), \ldots, u_n^{(m)}(t)\big)\,\mathrm{d}t \\
&+ \int_0^x K_2\big(x, t, u_1(t), \ldots, u_1^{(m)}(t), \ldots, u_n(t), \ldots, u_n^{(m)}(t)\big)\,\mathrm{d}t, \\
&\vdots \\
&u_n^{(m)}(x) = \\
&H_n\big(x, u_1(x), \ldots, u_1^{(m)}(x), \ldots, u_{n-1}(x), \ldots, u_{n-1}^{(m)}(x)\big) \\
&+ \int_a^b W_n\big(x, t, u_1(t), \ldots, u_1^{(m)}(t), \ldots, u_n(t), \ldots, u_n^{(m)}(t)\big)\,\mathrm{d}t
\end{aligned}$$

$$+\int_0^x K_n\big(x,t,u_1(t),\ldots,u_1^{(m)}(t),\ldots,u_n(t),\ldots,u_n^{(m)}(t)\big)\mathrm{d}t, \qquad (1)$$

In system (1), m is the order of derivatives and the continuous several variables functions H_i, W_i, and K_i, $i=1,2,\ldots,n$ are given, the solutions to be determined are $u_i(x)$, $i=1,2,\ldots,n$. In Section 2, the basic ideas of the homotopy analysis method are stated. Four examples are given in Section 3 to show efficiency and high accuracy of this method. Finally, conclusions are stated in Section 4.

2. Outline of Homotopy Analysis Method

To illustrate the basic concept of the homotopy analysis method, we consider the following general nonlinear system:

$$\mathcal{N}[u(r,t)]=0, \qquad (2)$$

where $\mathcal{N}$ is a nonlinear operator, $u(r,t)$ is an unknown function, and r and t denote spatial and temporal independent variables, respectively. For simplicity, we ignore all boundary or initial conditions, which can be treated in a similar way. By means of generalizing the traditional homotopy method, Liao [2] constructs the so-called zero-order deformation equation

$$(1-p)\mathcal{L}[\phi(r,t;p)-u_0(r,t)]=p\hbar\mathcal{H}(r,t)\mathcal{N}[\phi(r,t;p)], \qquad (3)$$

where $p\in[0,1]$ is the embedding parameter, $\hbar\neq 0$ the convergence-control parameter [30], $\mathcal{H}(r,t)\neq 0$ an auxiliary function, $\mathcal{L}$ an auxiliary linear operator, $u_0(r,t)$ an initial guess of $u(r,t)$, and $\phi(r,t;p)$ an unknown function, respectively. It is important that one has great freedom to choose auxiliary things in HAM. Obviously, when $p=0$ and $p=1$, it holds

$$\phi(r,t;0)=u_0(r,t), \quad \phi(r,t;1)=u(r,t),$$

respectively. Thus as p increases from 0 to 1, the solution $\phi(r,t;p)$ varies from the initial guess $u_0(r,t)$ to the solution $u(r,t)$. Expanding $\phi(r,t;p)$ in Taylor series with respect to p, one has

$$\phi(r,t;p)=u_0(r,t)+\sum_{m=1}^{+\infty}u_m(r,t)p^m, \qquad (4)$$

where

$$u_m(r,t)=\frac{1}{m!}\frac{\partial^m\phi(r,t;p)}{\partial p^m}\Big|_{p=0}. \qquad (5)$$

If the auxiliary linear operator, the initial guess, the convergence-control parameter $\hbar$, and the auxiliary function are so properly chosen, that the series (4) converges at $p=1$, one has

$$u(r,t)=u_0(r,t)+\sum_{m=1}^{+\infty}u_m(r,t),$$

which must be one of the solutions of the original nonlinear equation, as proved by Liao [2]. According to the definition (5), the governing equation can be deduced from the zero-order deformation equation (3). Define the vector

$$\vec{u}_n=\{u_0(r,t),u_1(r,t),\ldots,u_n(r,t)\}.$$

Differentiating (3) m times with respect to the embedding parameter p and then setting $p=0$ and finally dividing them by $m!$, we have the so-called mth-order deformation equation

$$\mathcal{L}[u_m(r,t)-\chi_m u_{m-1}(r,t)]=\hbar\mathcal{H}(r,t)R_m(\vec{u}_{m-1}), \qquad (6)$$

where

$$R_m(\vec{u}_{m-1})=\frac{1}{(m-1)!}\frac{\partial^{m-1}\mathcal{N}[\phi(r,t;p)]}{\partial p^{m-1}}\Big|_{p=0} \qquad (7)$$

and

$$\chi_m=\begin{cases}0, & m\leq 1,\\ 1, & m>1.\end{cases}$$

It should be emphasized that $u_m(r,t)$ for $m>1$ is governed by the linear equation (6) with the linear boundary conditions that come from the original problem, which can be easily solved by symbolic computation software such as Maple and Mathematica.

3. Applications

In this section, we present some examples to show efficiency and high accuracy of the homotopy analysis method for solving system of integro-differential equations (1).

Example 3.1 Let us first consider a system of integro-differential equations as follows:

$$\begin{aligned}
&u'(x)=xv(x)+\sin x-x+\int_0^{\frac{\pi}{2}}xu(t)\mathrm{d}t,\\
&v'''(x)=+\sin x-x+\int_0^{\frac{\pi}{2}}xu(t)\mathrm{d}t,\\
&u(0)=0, \quad v(0)=1, \quad v'(0)=0, \quad v''(0)=-1,
\end{aligned}$$

with the exact solutions

$$u(x) = x\sin x, \quad v(x) = \cos x.$$

According to the section before, we assume that the solution of the system, $u(t)$ and $v(t)$, can be expressed by the following set of base functions:

$$\{x^p, x^m \sin x, x^n \cos x \,|\, m, n, p = 0, 1, 2, 3, \ldots\}.$$

We choose the linear operators

$$\mathcal{L}_1[\phi_i(x;p)] = \frac{\partial \phi_i(x;p)}{\partial x}, \quad \mathcal{L}_2[\phi_i(x;p)] = \frac{\partial^3 \phi_i(x;p)}{\partial x^3}, \quad i = 1, 2$$

with the property

$$\mathcal{L}_1[c_0] = 0, \quad \mathcal{L}_2[c_0 + c_1 x + c_2 x^2] = 0,$$

where c_i, $i = 0, 1, 2$ are constant. We define the non-linear operators

$$\mathcal{N}_1[\phi_1(x;p), \phi_2(x;p)] = \frac{\partial \phi_1(x;p)}{\partial x} - x\phi_2(x;p) - \sin x + x - \int_0^{\frac{\pi}{2}} x\phi_1(t;p)\mathrm{d}t,$$

$$\mathcal{N}_2[\phi_1(x;p), \phi_2(x;p)] = \frac{\partial^3 \phi_1(x;p)}{\partial x^3} - \sin x + x - \int_0^{\frac{\pi}{2}} x\phi_1(t;p)\mathrm{d}t.$$

We choose the auxiliary function $\mathcal{H}(x) = -1$ for simplicity and $\phi_1(x;0) = u_0(x) = 0$ and $\phi_2(x;0) = v_0(x) = -\frac{1}{2}x^2 + 1$ which satisfy the initial conditions. Hence, the high-order deformation equations are:

$$\begin{aligned} &\mathcal{L}_1[u_m(x) - \chi_m u_{m-1}(x)] = -\hbar R_m(\vec{u}_{m-1}), \\ &\mathcal{L}_2[v_m(x) - \chi_m v_{m-1}(x)] = -\hbar S_m(\vec{v}_{m-1}) \end{aligned} \tag{8}$$

with the boundary conditions

$$u_m(0) = 0, \quad v_m(0) = v'_m(0) = v''_m(0) = 0,$$

where

$$\begin{aligned} R_m(\vec{u}_{m-1}) = {} & u'_{m-1}(x) - x v_{m-1}(x) \\ & - (1-\chi_m)(\sin x - x) - \int_0^{\frac{\pi}{2}} x u_{m-1}(t)\mathrm{d}t, \\ S_m(\vec{u}_{m-1}) = {} & v'''_{m-1}(x) - (1-\chi_m)(\sin x - x) \\ & - \int_0^{\frac{\pi}{2}} x u_{m-1}(t)\mathrm{d}t. \end{aligned}$$

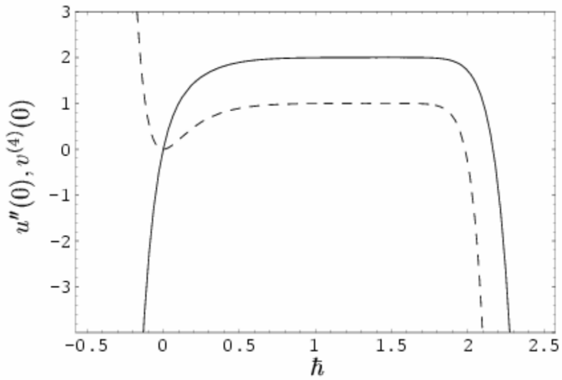

Fig. 1. $\hbar$-curves; solid line: 15th-order approximation of $u''(0)$; dashed line: 15th-order approximation of $v^{(4)}(0)$.

(a)

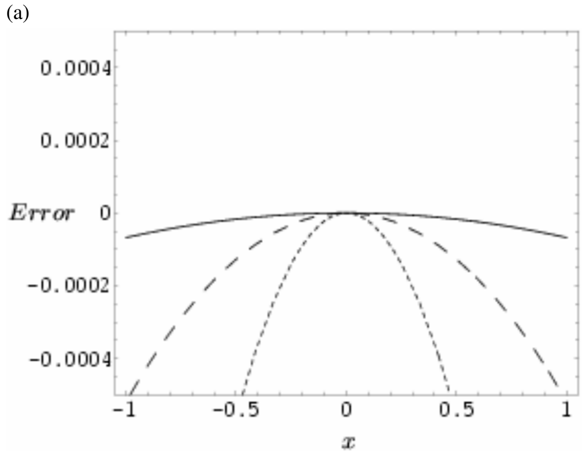

(b)

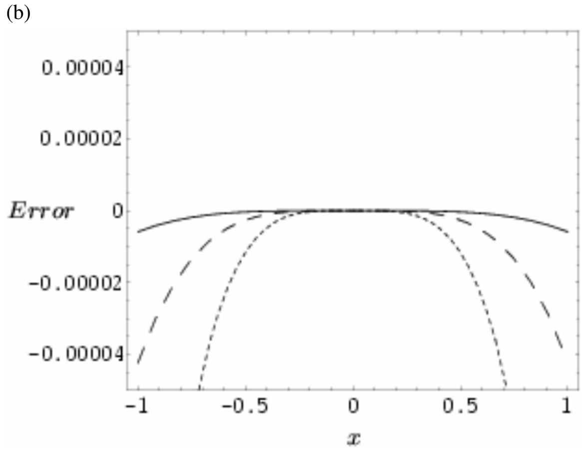

Fig. 2. (a) Error of 15th-order approximate solution $U_M(x)$; solid line: $\hbar = 1.45$; dashed line: $\hbar = 1.2$; dotted line: $\hbar = 1$. (b) Error of 15th-order approximate solution $V_M(x)$; solid line: $\hbar = 1.45$; dashed line: $\hbar = 1.2$; dotted line: $\hbar = 1$.

Now, we can obtain $u_i(x)$ and $v_i(x)$ for $i = 1,2,\ldots$ successively by solving the system of ordinary differential equations (8), and then by choosing a proper convergence-control parameter $\hbar$ we receive $U_M(x) = \sum_{i=1}^{M} u_i(x)$ and $V_M(x) = \sum_{i=1}^{M} v_i(x)$ as analytic approximate solutions. To show the influence of $\hbar$ on the convergence of $U_M(x) = \sum_{i=1}^{M} u_i(x)$ and $V_M(x) = \sum_{i=1}^{M} v_i(x)$, we first plot the so-called $\hbar$-curves of $u''(0)$ and $v^{(4)}(0)$ as shown in Figure 1. It is easy to discover the valid region of the convergence-control parameter $\hbar$. Also, the error function $U_M(x) = \sum_{i=1}^{M} u_i(x)$ and $V_M(x) = \sum_{i=1}^{M} v_i(x)$ i. e. $|x\sin x - U_M(x)|$ and $|\cos x - V_M(x)|$ with $M = 15$ are shown for different convergence-control parameter $\hbar$ in Figure 2.

Example 3.2 [31] Let us consider the following nonlinear system of one integro-differential equation

$$u'''(x) = \sin x - x - \int_0^{\frac{\pi}{2}} xtu'(t)\mathrm{d}t,$$
$$u(0) = 1, \quad u'(0) = 0, \quad u''(0) = 1,$$

with the exact solution

$$u(x) = \cos x.$$

We choose the auxiliary function, the auxiliary linear operator, the initial guess, and the nonlinear operator, respectively, as follows:

$$\mathcal{H}(x) = -1,$$
$$\mathcal{L}[\phi(x;p)] = \frac{\partial^3\phi(x;p)}{\partial x^3}$$
with the property $\mathcal{L}[c_0 + c_1x + c_2x^2] = 0$,
$$\phi(x;0) = u_0(x) = -\frac{1}{2}x^2 + 1,$$
$$\mathcal{N}[\phi(x;p)] = \frac{\partial^3\phi(x;p)}{\partial^3 x} - \sin(x) + x + \int_0^{\frac{\pi}{2}}\left(xt\frac{\partial\phi(t;p)}{\partial t}\right)\mathrm{d}t.$$

We notice that the initial guess satisfies the initial conditions, therefore the high-order deformation equation is

$$\mathcal{L}[u_m(x) - \chi_m u_{m-1}(x)] = \hbar R_m(\vec{u}_{m-1})$$

with the boundary conditions

$$u_m(0) = u'_m(0) = u''_m(0) = 0,$$

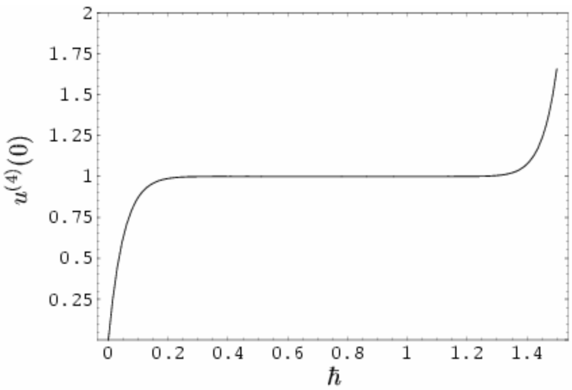

Fig. 3. $\hbar$-curves; 15th-order approximation of $u^{(4)}(0)$.

(a)

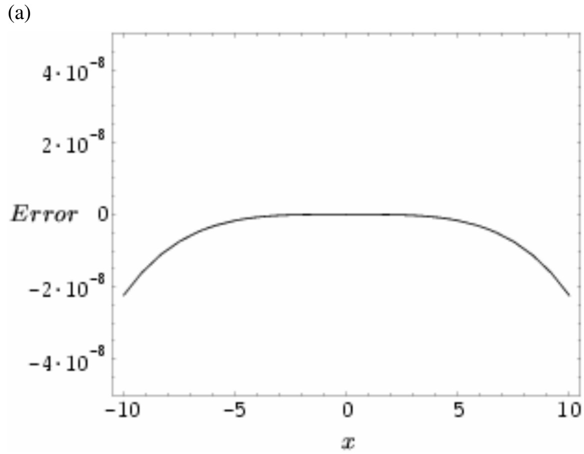

(b)

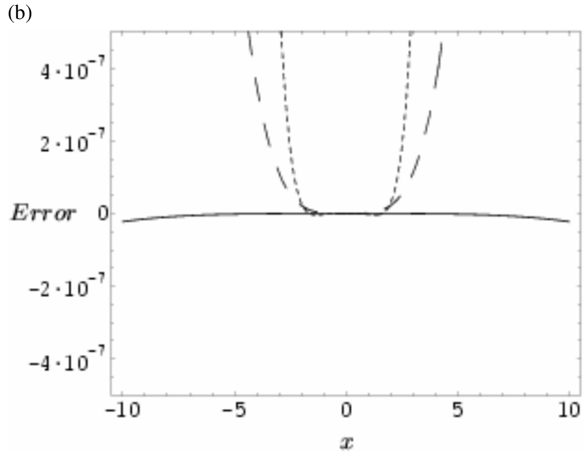

Fig. 4. (a) Error of 15th-order approximate solution $U_M(x)$ with $\hbar = 0.8$; (b) error of 15th-order approximate solution $U_M(x)$; solid line: $\hbar = 0.8$; dotted line: $\hbar = 0.6$; dashed line: $\hbar = 1$.

where

$$R_m(\vec{u}_{m-1}) = u'''_{m-1}(x) - (1-\chi_m)(\sin(x) - x) + \int_0^{\frac{\pi}{2}} xt u'_{m-1}(t)\mathrm{d}t.$$

In Figure 3, the $\hbar$-curve of $u^{(4)}(0)$ has been shown (notice that the $u'''(0)$ is constant in the form of an approximate series solution and it is not useful to gain valid region of convergence-control parameter $\hbar$). The error function $|\cos x - U_M(x)|$ is shown in Figure 4a. We compared error functions with different $\hbar$ in Figure 4b and we can see from these figures that this method is highly promising.

Example 3.3 Consider the following nonlinear system of two integro-differential equations:

$$u'(x) = v'(x) + \frac{1}{4}x - \frac{1}{4}\int_0^{\frac{\pi}{2}} xtv(t)\mathrm{d}t,$$
$$v''(x) = -u(x) + x - \int_0^{\frac{\pi}{2}} xtu(t)\mathrm{d}t,$$
$$u(0) = 0, \quad v(0) = 0, \quad v'(0) = 1$$

with the exact solutions

$$u(x) = \sin x, \quad v(x) = \sin x.$$

For this example, the auxiliary functions, the auxiliary linear operators, the initial guesses and the nonlinear operators are chosen, respectively, as follows:

$$\mathcal{H}(x) = -1,$$
$$\mathcal{L}_1[\phi_i(x;p)] = \frac{\partial \phi_i(x;p)}{\partial x}, \quad i = 1,2$$
with the property $\mathcal{L}_1[c_0] = 0$,
$$\mathcal{L}_2[\phi_i(x;p)] = \frac{\partial^2 \phi_i(x;p)}{\partial x^2}, \quad i = 1,2$$
with the property $\mathcal{L}_2[c_0 + c_1 x] = 0$,
$$\phi_1(x;0) = u_0(x) = 0, \quad \phi_2(x;0) = v_0(x) = x,$$

$$\mathcal{N}_1[\phi_1(x;p), \phi_2(x;p)] = \frac{\partial \phi_1(x;p)}{\partial x} - \frac{\partial \phi_2(x;p)}{\partial x} - \frac{1}{4}x + \frac{1}{4}\int_0^{\frac{\pi}{2}} xt\phi_2(t;p)\mathrm{d}t,$$

$$\mathcal{N}_2[\phi_1(x;p), \phi_2(x;p)] = \frac{\partial^2 \phi_2(x;p)}{\partial x^2} + \phi_1(x;p) - x + \int_0^{\frac{\pi}{2}} xt\phi_1(t;p)\mathrm{d}t.$$

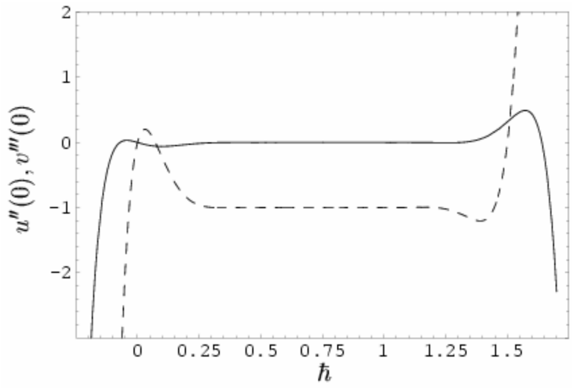

Fig. 5. $\hbar$-curves; solid line: 15th-order approximation of $u''(0)$; dashed line: 15th-order approximation of $v'''(0)$.

(a)

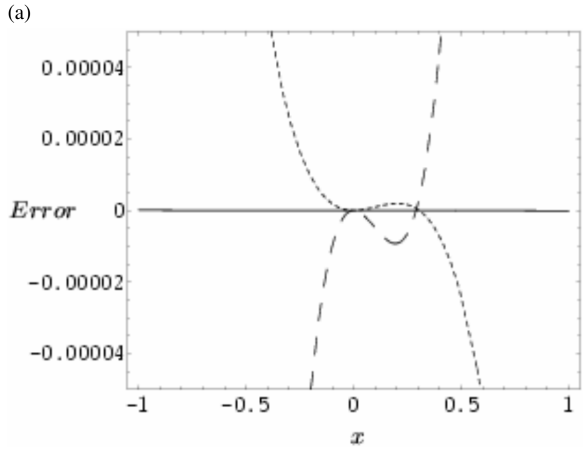

(b)

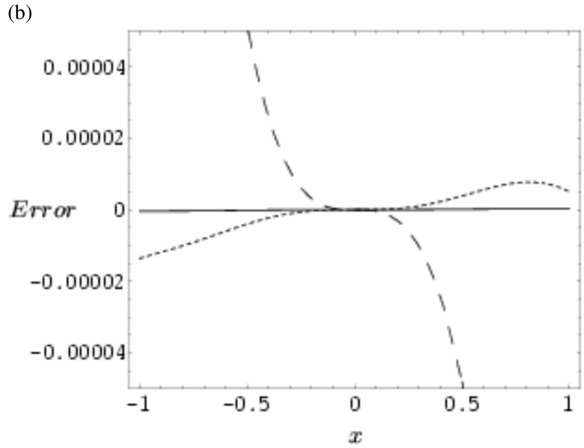

Fig. 6. (a) Error of 10th-order approximate solution $U_M(x)$; dotted line: $\hbar = 0.80$; solid line: $\hbar = 0.90$; dashed line: $\hbar = 1$; (b) error of 10th-order approximate solution $V_M(x)$; dotted line: $\hbar = 0.70$; solid line: $\hbar = 0.83$; dashed line: $\hbar = 1$. (Example 3.3).

(a)

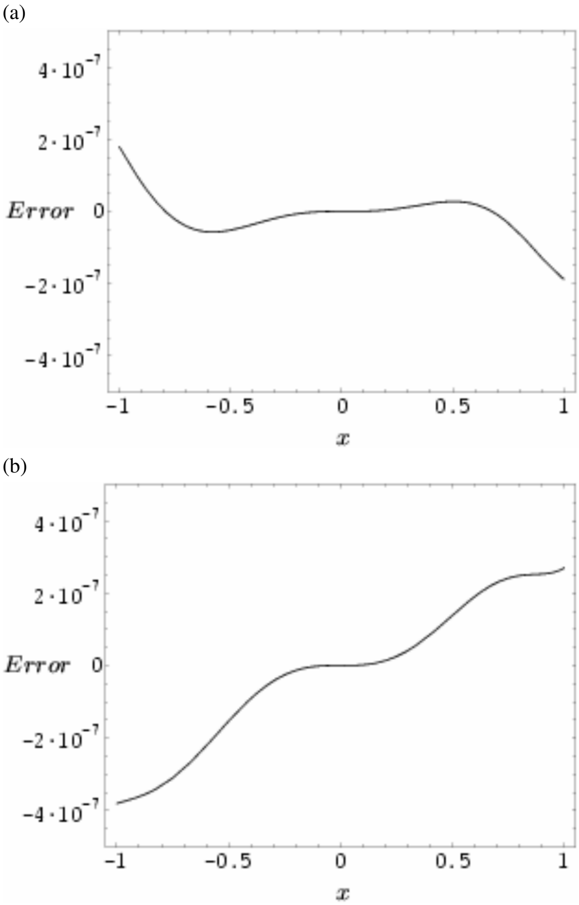

Fig. 7. (a) Error of 10th-order approximate solution $U_M(x)$ with $\hbar = 0.90$; (b) error of 10th-order approximate solution $V_M(x)$ with $\hbar = 0.83$.

The high-order deformation equations are

$$\mathcal{L}_1[u_,(x) - \chi_m u_{m-1}(x)] = -\hbar R_m(\vec{u}_{m-1}),$$
$$\mathcal{L}_2[v_,(x) - \chi_m v_{m-1}(x)] = -\hbar S_m(\vec{v}_{m-1})$$

with the boundary conditions

$$u_m(0) = 0, \quad v_m(0) = 0, \quad v'_m(0) = 0,$$

where

$$R_m(\vec{u}_{m-1}) = u'_{m-1}(x) - v'_{m-1}(x) - \frac{1}{4}(1-\chi_m)x + \frac{1}{4}\int_0^{\frac{\pi}{2}} xtv_{m-1}(t)\mathrm{d}t,$$

$$S_m(\vec{v}_{m-1}) = v''_{m-1}(x) - u_{m-1}(x) - (1-\chi_m)x + \int_0^{\frac{\pi}{2}} xtu_{m-1}(t)\mathrm{d}t.$$

In Figure 5, the $\hbar$-curves of $u''(0)$ and $v'''(0)$ are shown. We also plotted the error functions $|\sin x - U_M(x)|$ and $|\sin x - V_M(x)|$ with $M = 15$ for different $\hbar$ in Figure 6. Also, separately, the error of 10th-order approximate solution $U_M(x)$ and $V_M(x)$ with $\hbar = 0.90$ and $\hbar = 0.83$, respectively, have been shown in Figure 7.

Example 3.4 [32] Now, let us test the homotopy analysis method on the following linear system of two Volterra's integro-differential equations:

$$u'(x) = 1 + x + x^2 - v(x) - \int_0^x (u(t) + v(t))\mathrm{d}t,$$
$$v'(x) = -1 - x + u(x) - \int_0^x (u(t) - v(t))\mathrm{d}t$$

with the initial conditions

$$u(0) = 1, \quad v(0) = -1,$$

and with the exact solutions

$$u(x) = x + \mathrm{e}^x, \quad v(x) = x - \mathrm{e}^x.$$

Here, we choose the auxiliary functions, the auxiliary linear operators, the initial guesses and the nonlinear operators, respectively, as follows:

$$\mathcal{H}(x) = -1,$$
$$\mathcal{L}[\phi_i(x;p)] = \frac{\partial \phi_i(x;p)}{\partial x}, \quad i = 1,2$$

with the property $\mathcal{L}[c_0] = 0$,

$$\phi_1(x;0) = u_0(x) = 1, \quad \phi_2(x;0) = v_0(x) = -1,$$
$$\mathcal{N}_1[\phi_1(x;p), \phi_2(x;p)] = \frac{\partial \phi_1(x;p)}{\partial x} - 1 - x - x^2 + \phi_2(x;p) + \int_0^x [\phi_1(x;p) + \phi_2(x;p)]\mathrm{d}t,$$

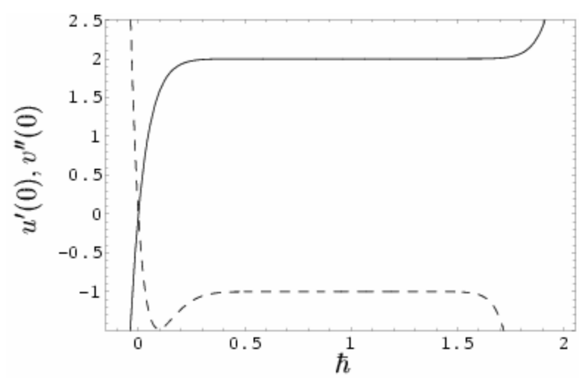

Fig. 8. $\hbar$-curves; solid line: 15th-order approximation of $u'(0)$; dashed line: 15th-order approximation of $v''(0)$.

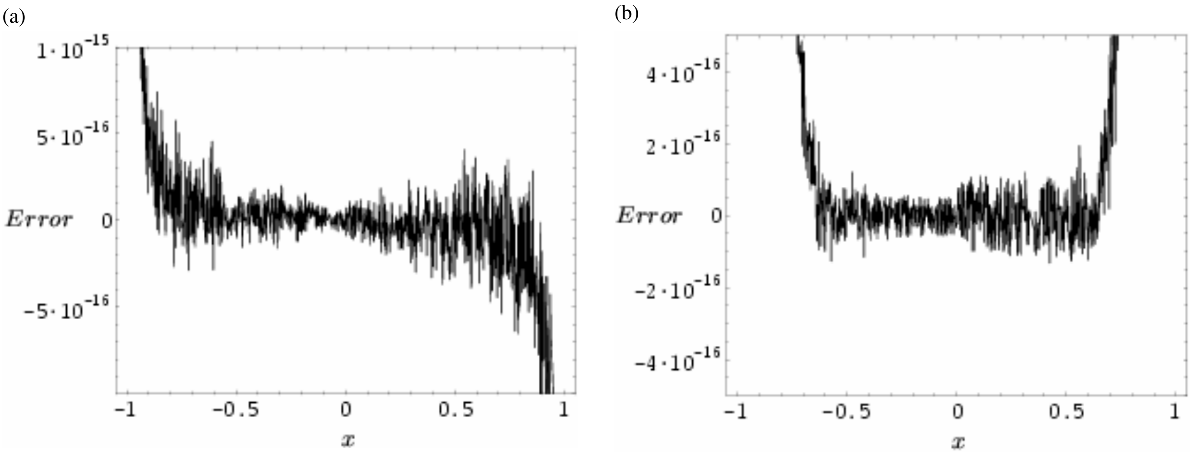

Fig. 9. (a) Error of 15th-order approximate solution $U_M(x)$ with $\hbar = 1$; (b) The error of 15th-order approximate solution $V_M(x)$ with $\hbar = 1$.

$$\mathcal{N}_2[\phi_1(x;p),\phi_2(x;p)] = \frac{\partial \phi_2(x;p)}{\partial x} + 1 + x - \phi_1(x;p) + \int_0^x [\phi_1(x;p) - \phi_2(x;p)]\mathrm{d}t.$$

The high-order deformation equations are:

$$\mathcal{L}[u_m(x) - \chi_m u_{m-1}(x)] = -\hbar R_m(\vec{u}_{m-1}),$$
$$\mathcal{L}[v_m(x) - \chi_m v_{m-1}(x)] = -\hbar S_m(\vec{v}_{m-1})$$

with the boundary conditions

$$u_m(0) = 0, \quad v_m(0) = 0,$$

where

$$R_m(\vec{u}_{m-1}) = u'_{m-1}(x) - (1-\chi_m)(1+x+x^2) + v_{m-1}(x) + \int_0^x (u_{m-1}(t) + v_{m-1}(t))\mathrm{d}t,$$
$$S_m(\vec{v}_{m-1}) = v'_{m-1}(x) + (1-\chi_m)(1+x) - u_{m-1}(x) + \int_0^x (u_{m-1}(t) - v_{m-1}(t))\mathrm{d}t.$$

As in the previous examples, the $\hbar$-curves and the error functions have been plotted in Figures 8 and 9, respectively.

4. Conclusions

In this paper, we have studied some systems of linear and nonlinear integro-differential equations with the help of homotopy analysis method. The results showed that the HAM is remarkably effective for these problems.

Acknowledgements

The authors would like to thank the anonymous referees for their helpful comments.

[1] S. J. Liao, The proposed homotopy analysis techniques for the solution of nonlinear problems, PhD dissertation, Shanghai Jiao Tong University, 1992 (in English).
[2] S. J. Liao, Beyond Perturbation: Introduction to the Homotopy Analysis Method, Chapman Hall CRC/Press, Boca Raton 2003.
[3] T. Hayat and M. Sajid, Phys. Lett. A **361**, 31622 (2007).
[4] T. Hayat and M. Sajid, Int. J. Heat. Mass Transf **50**, 7584 (2007).
[5] S. Abbasbandy, Nonlinear Dyn. **51**, 837 (2008).
[6] S. Abbasbandy, Phys. Lett. A **361**, 47883 (2007).
[7] S. Abbasbandy, Phys. Lett. A **360**, 10913 (2006).
[8] S. Abbasbandy, Int. Commun. Heat Mass Transf. **34**, 3807 (2007).
[9] S. P. Zhu, Quantitative Finance **6**, 22941 (2006).
[10] S. P. Zhu, Anziam J. **47**, 47794 (2006).
[11] Y. Wu and K. F. Cheung, Int. J. Numer. Meth. Fluids, **57**, 1649 (2008).
[12] M. Yamashita, K. Yabushita, and K. Tsuboi, J. Phys. A **40**, 840316 (2007).
[13] Y. Bouremel, Commun. Nonlinear Sci. Numer. Simul. **12**, 71424 (2007).

[14] L. Tao, H. Song, and S. Chakrabarti, Clastal. Eng. **54**, 82534 (2007).
[15] H. Song and L. Tao, J. Coastal. Res. **50**, 2925 (2007).
[16] A. Molabahrami and F. Khani, Nonlinear Anal. B: Real World Appl. **10**, 589 (2009).
[17] A. S. Bataineh, M. S. M. Noorani, and I. Hashim, Phys. Lett. A **371**, 7282 (2007).
[18] Z. Wang, L. Zou, and H. Zhang, Phys. Lett. A **369**, 7784 (2007).
[19] M. Inc, Phys. Lett. A **365**, 41215 (2007).
[20] W. H. Cai, Nonlinear Dynamics of thermal-hydraulic networks, PhD thesis, University of Notre Dame, Indiana 2006.
[21] S. Abbasbandy, Appl. Math. Model **32**, 2706 (2008).
[22] H. Wang, H. M. Fu, and H. F. Zhang, Int. J. Nonlinear Sci. Numer. Simul. **8**, 171 (2007).
[23] L. Xu, J. H. He, and Y. Liu, Int. J. Nonlinear Sci. Numer. Simul. **8**, 199 (2007).
[24] F. Z. Sun, M. Gao, S. H. Lei, Y. B. Zhao, K. Wang, Y. T. Shi, and N. H. Wang, Int. J. Nonlinear Sci. Numer. Simul. **8**, 211 (2007).
[25] T. L. Bo, L. Xie, and X. J. Zheng, Int. J. Nonlinear Sci. Numer. Simul. **8**, 223 (2007).
[26] S. M. El-Sayed, D. Kaya, and S. Zarea, Int. J. Nonlinear Sci. Numer. Simul. **5**, 105 (2004).
[27] J. Saberi-Nadjafi and M. Tamamgar, Comput. Math. Appl. **56**, 346 (2008).
[28] J. Biazar, H. Ghazvini, and M. Eslami, Chaos, Solitons, and Fractals **39**, 1253 (2008).
[29] J. Biazar, Appl. Math. Comput. **168**, 1232 (2005).
[30] S. J. Liao, Commun. Nonlinear Sci. Numer. Simul. **14**, 983 (2009).
[31] A. Golbabai, and M. Javidi, Appl. Math. Comput. **190**, 1409 (2007).
[32] E. Yusufoğlu, Appl. Math. Comput. **192**, 51 (2007).